JOURNAL OF NEUROTRAUMA 27:2067–2076 (November 2010)

DOI: 10.1089/neu.2010.1403

Sustained Expression of Vascular Endothelial Growth Factor and Angiopoietin-1 Improves Blood–Spinal Cord Barrier Integrity and Functional Recovery after Spinal Cord Injury

Juan J. Herrera,[1] Laura M. Sundberg,[1] Lorena Zentilin,[2] Mauro Giacca,[2,3] and Ponnada A. Narayana[1]

Abstract

Spinal cord injury (SCI) results in immediate disruption of the spinal vascular network, triggering an ischemic environment and initiating secondary degeneration. Promoting angiogenesis and vascular stability through the induction of vascular endothelial growth factor (VEGF) and angiopoietin-1 (Ang-1), respectively, provides a possible therapeutic approach in treating SCI. We examined whether supplementing the injured environment with these two factors, which are significantly reduced following injury, has an effect on lesion size and functional outcome. Sustained delivery of both $VEGF_{165}$ and Ang-1 was realized using viral vectors based on the adeno-associated virus (AAV), which were injected directly into the lesion epicenter immediately after injury. Our results indicate that the combined treatment with VEGF and Ang-1 resulted in both reduced hyperintense lesion volume and vascular stabilization, as determined by magnetic resonance imaging (MRI). Western blot analysis indicated that the viral vector expression was maintained into the chronic phase of injury, and that the use of the AAV vectors did not exacerbate infiltration of microglia into the lesion epicenter. The combined treatment with AAV-VEGF and AAV-Ang-1 improved locomotor recovery in the chronic phase of injury. These results indicate that combining angiogenesis with vascular stabilization may have potential therapeutic applications following SCI.

Key words: angiopoietin-1; magnetic resonance imaging; traumatic spinal cord injury; vascular endothelial growth factor; viral mediated transfection

Introduction

Traumatic spinal cord injury (SCI) triggers an immediate disruption of the spinal cord vasculature that results in secondary damage induced by the activation of a cascade of cellular and molecular changes, such as cellular excitotoxicity, increased tissue edema, free radical production, cytokine and chemokine production, and inflammation (Fehlings et al., 1989; Hausmann, 2003). The compromised spinal cord circulation at the injury site contributes to ischemia and impairs repair processes after injury (Tator, 1991). Previous studies have also demonstrated that disruption of spinal cord blood flow is related to the motor and sensory deficits that result from spinal cord injury (Holtz et al., 1990; Lang-Lazdunski et al., 2000; Patel et al., 2009; Tator and Fehlings, 1991).

Two key proteins that regulate the angiogenic response and vascular stability are the 165-amino-acid isoform of the vascular endothelial growth factor-A gene (herein referred to as $VEGF_{165}$ for brevity), and angiopoietin-1 (Ang-1). VEGF is a potent stimulator of endothelial cell proliferation, migration, and survival (Neufeld et al., 1999). In addition, VEGF is also known for its neurotrophic, neuroprotective, and neuroproliferative effects after injury (Greenberg and Jin, 2005; Harrigan et al., 2003; Hayashi et al., 1998; Kaya et al., 2005; Sun et al., 2003). We have recently reported a significant decrease in the $VEGF_{165}$ isoform after injury (Herrera et al., 2009). Consistent with these findings, other recent publications have indicated that induction of VEGF signaling through gene therapeutic approaches reduces lesion volume and enhances functional recovery after SCI (Liu et al., 2010). However, increased VEGF is known to induce profound leakage of endothelial cells *in vitro* and adult microvasculature *in vivo* (Ferrara et al., 2003), and it is well established that the increase in vascular permeability induced by VEGF plays an important role in inducing inflammation in the central nervous system (CNS) (Croll et al., 2004; Proescholdt et al., 2002; Suidan et al., 2010).

[1]Department of Diagnostic and Interventional Imaging, The University of Texas Health Science Center at Houston, Houston, Texas.
[2]Molecular Medicine Laboratory, International Centre for Genetic Engineering and Biotechnology (ICGEB), Trieste, Italy.
[3]Department of Biomedicine, Faculty of Medicine, University of Trieste, Trieste, Italy.

In contrast to $VEGF_{165}$ as a promoter of angiogenesis, Ang-1 plays an important role in vascular remodeling, maturation, and stabilization (Davis et al., 1996; Suri et al., 1996). It has been demonstrated that administration of Ang-1 reduces vascular permeability and lesion volume after ischemic injury (Zhang et al., 2002a). Thurston and associates showed that systemic Ang-1 production by adenoviral gene delivery resulted in reduced vascular leakage induced by VEGF (Thurston et al., 2000), or inflammatory agents (Thurston et al., 1999). A recent study by Han and colleagues indicated that intravenous delivery of Ang-1 had protective effects after SCI (Han et al., 2010).

Combination therapy with both $VEGF_{165}$ and Ang-1 may be a promising approach in promoting the angiogenic response, while creating more stable vessel formation in the ischemic environment after SCI. The sustained delivery of both factors has been achieved using adeno-associated viral vectors (AAV) in models of stroke and cardiovascular disease (Arsic et al., 2003; Zacchigna et al., 2007; Zhao et al., 2009). AAV vectors offer significant advantages over other viral-based delivery systems. AAV vectors can transduce target cells at a high multiplicity of infection, and do not generate the inflammatory responses observed with other viral delivery systems (Hermens and Verhaagen, 1998). Zhao and associates demonstrated that combined Ang-1 and VEGF gene therapy in cerebral ischemia promoted vascular stabilization and neuroprotection without the side effects of increased blood–brain barrier permeability (Zhao et al., 2009).

In the current study we determined the protein expression profile of Ang-1 after SCI, and examined the effects of acute AAV-$VEGF_{165}$ and AAV-Ang-1 treatments after SCI. We report that combined treatment with $VEGF_{165}$ and Ang-1 resulted in increased expression of both proteins in the chronic phase of injury, contributing to reduced lesion volume and improved blood–spinal cord barrier (BSCB) integrity as assessed using magnetic resonance imaging (MRI). Our results also showed that the use of AAV vectors did not exacerbate the inflammatory response after injury.

Methods

Production, purification, and characterization of recombinant AAV vectors

Viral vectors were generated and characterized as described previously (Arsic et al., 2003; Bitto et al., 2008; Zacchigna et al., 2007). Briefly, three viral recombinant AAV serotype 8 vectors were used in this study, engineered to express the LacZ reporter gene, the 165-amino-acid isoform of the VEGF-A gene, or Ang-1 under the control of the constitutive cytomegalovirus (CMV) immediate–early promoter. The vector stock titers ranged from $\sim 1\times10^{12}$ to $\sim 1\times10^{13}$ viral genome copies per milliliter.

Animals, spinal cord injury procedure, and intraspinal microinjection for viral administration

The protocol used in this study was reviewed and approved by the Institutional Animal Welfare Committee. The guidelines provided in the National Institutes of Health (NIH) Guide for the Care and Use of Laboratory Animals were strictly followed.

A total of 48 adult male Sprague-Dawley rats weighing between 300 and 350 g were used in these studies. Spinal cord injuries were produced as described previously (Herrera et al., 2009). The animals were anesthetized with 4% isoflurane and maintained under anesthesia with a mixture of 2% isoflurane, air, and oxygen, administered through a Harvard rodent ventilator (Model 683; Harvard Apparatus, Holliston, MA) during the entire procedure. A laminectomy was performed at the seventh thoracic vertebra (T7) and a 150-kDyn force with a 1-sec dwell time was delivered to the exposed cord using an Infinite Horizon Impactor (Precision Systems and Instrumentation, Lexington, KY) to produce a moderate level of injury.

For improved signal-to-noise ratio (SNR) and MRI image quality, an 11×35-mm rectangular radio frequency (RF) coil was implanted over the spinal column and centered on the site of injury (Deo et al., 2006; Fenyes and Narayana, 1998). The implanted coil was held in place with two sutures and tuned to 300 MHz, the MRI scanner frequency. The overlying paraspinal muscles were then sutured at the midline and the skin was closed. For intravenous delivery of contrast agent, the right jugular vein was cannulated and a vascular port with silicone tubing was placed (Instech Solomon, Plymouth Meeting, PA) as described previously (Patel et al., 2009). Briefly, the vascular port was implanted subcutaneously on the ventral side of the animal above the right pectoral muscle and the incision was closed. To ensure patency of the jugular port and connected tubing during the 28 and 56 days post-injury, 0.2 mL of 0.9% saline was injected into the port before and after each scan. If resistance was felt on the plunger of the syringe during administration of the saline bolus, the port or tubing was assumed to be blocked and the animal was excluded from further MRI scanning. Final confirmation of patency of the jugular port was assessed after the T1-weighted post-contrast scan, in which the presence of contrast agent could be readily observed in the vasculature.

The animals were allowed to recover in warmed cages and received subcutaneous injections of Cefazolin (11 mg/kg; Butler Schein Animal Health Supply, Dublin, OH) twice a day for 10 days, and buprenorphine (0.01 mg/kg; Hospira, Inc., Lake Forest, IL) twice a day for 5 days. The animals were also administered subcutaneous injections of saline twice daily for 5 days. The animals' bladders were manually expressed twice daily until the return of spontaneous urination. The animals had free access to food and water.

For sustained expression of $VEGF_{165}$ and/or Ang-1, the animals received a total of 2.0 μL of AAV-$VEGF_{165}$/Ang-1 injected directly into the lesion epicenter at a depth of 1 mm from the surface of the spinal cord. Animals receiving AAV-$VEGF_{165}$, AAV-Ang-1, or AAV-LacZ alone were injected with 1 μL of the virus mixed with 1 μL of saline ($n = 6$/time point). This was performed to maintain consistent volumes across all groups. The AAV constructs were delivered using glass micropipettes with an inner diameter of 40 μm and Picospritzer II apparatus (Parker Hannifin Corporation, Farifield, NJ). The micropipette was left in the cord for 3 min to avoid backflow.

Magnetic resonance imaging to determine lesion volume

All MRI studies were carried out on an actively shielded Bruker Biospec 70/30 URS scanner operating at a field strength of 7 T (Bruker Biospec, Karlsruhe, Germany). A 15×30-mm external coil was placed under the animal's back

and inductively coupled to the implanted RF coil. The respiratory rate and rectal temperature were monitored throughout the experiment with a physiologic monitoring unit (Model 1025; SA Instruments, Inc., Stonybrook, NY). A pulse oximeter (Model 8600V; Nonin Medical Inc., Plymouth, MN) was used to monitor heart rate and oxygen saturation levels. For the duration of the experiment, a heating system (Model 11007B; SA Instruments, Inc.) was used to maintain body temperature at 37°C. Respiratory gating was employed to minimize breathing artifacts in the images. High-resolution rapid acquisition by relaxation enhancement (RARE) images were acquired using the following parameters: rare factor of 4, TE1/TE2/TR = 21.2/63.6/3150 msec, image matrix of 256×256, field of view of 2.62 cm, and 35 contiguous 1-mm-thick slices. Pre- and post-contrast T1-weighted images (acquisition parameters: TR = 500 msec and TE = 10.4 msec) were acquired with identical geometry as the RARE images.

Prior to all animal scans, MRI of a phantom study was performed to ensure scanner quality control and to assess SNR.

Evaluation of MRI lesion volume and blood–spinal cord permeability

The RARE scans provided high-resolution images of the injured spinal cord. The images exhibited both hyper- and hypointense lesions that represent edema/demyelination and hemorrhage/necrosis, respectively (Weirich et al., 1990). RARE images were analyzed for lesion quantification using Image-Pro Plus 5.1 software (Media Cybernetics, Inc., Silver Spring, MD). Threshold intensities were determined for both hypo- and hyperintense lesions by comparison with normal uninjured spinal cord tissue. Lesion volumes of the virally-treated groups were determined by applying the threshold levels obtained from normal animals to the region of interest encompassing the injured spinal cord. The total hypo- and hyperintense areas were recorded for each image slice. The total volumes for hypo- and hyperintense regions were calculated per treatment group and compared.

To assess the integrity of the BSCB, contrast-enhanced MRI was performed at 28 and 56 days post-injury, by intravenous administration of the paramagnetic contrast agent gadopentate dimeglumine (Gd, 287 mg/kg, Magnevist; Berlex Laboratories, Montville, NJ) through the implanted vascular access port connected to tubing that was catheterized to the jugular vein as described above (Cohen et al., 2009; Patel et al., 2009; Tofts et al., 1999). The contrast-enhanced data were objectively and quantitatively analyzed in an unbiased manner to estimate the area of enhancement in the injured cord as described elsewhere (Bilgen et al., 2001). The percentage of enhanced area in a slice, which reflects a compromised BSCB, was quantified from the region of interest (ROI) encompassing the spinal cord. The total percentage area was summed for each treatment group.

Behavioral tests

For chronic studies, each animal was evaluated at days 7, 14, 28, 42, and 56 post-SCI using the Basso-Beattie-Bresnahan open field locomotion scale (BBB scale) for testing hindlimb function (Basso et al., 1995). Injured animals were assessed 2 days following injury, and then once a week for 8 weeks as described previously (Scheff et al., 2003). Other neurobehavioral assays such the grid walk (Bresnahan et al., 1987), von Frey filament test (Peng et al., 2006), and inclined plane performance (Rivlin and Tator, 1977), and measures of activity using the Photobeam Activity System (PAS) with Flexfield (San Diego Instruments, Inc., San Diego, CA) computerized activity boxes (Mills et al., 2001) were also performed, but no significant differences were observed. The neurobehavioral assays listed require a larger number of animals per group to reach statistical significance. Power analysis for this study was performed with MRI measures as the main focus.

Western blot analysis of the Ang-1 profile after acute SCI

To the best of our knowledge, there is no published literature on the expression profile of Ang-1 after SCI. To assess the protein expression profile of Ang-1 in the acute phase post-SCI, we performed Western blot analysis at the lesion epicenter from injured animals ($n = 4$/time point), that were harvested at 6, 24, 48, and 72 h post-injury. Additional samples from 56-days post-injured tissue were also analyzed ($n = 4$). These samples were obtained from animals that underwent the same surgical procedure and post-operative care as mentioned previously (Herrera et al., 2009), and were processed the same way as the acute samples described below. Injured tissues were compared with normal intact controls ($n = 4$). Our previous study examined the expression profile of $VEGF_{165}$ in a similar manner following contusive SCI (Herrera et al., 2009).

Western blot analysis of viral vectors after intraspinal injection into the injured spinal cord

A total of 24 animals ($n = 6$/group) were used to assess the viral vector treatment following SCI. To determine the expression of viral vectors, samples from the lesion epicenter ($n = 3$/group) were harvested and processed as described previously (Herrera et al., 2009). Briefly, samples from the lesion epicenter containing 40 (g of protein were mixed with 6X super denaturing sample buffer (350 mM Tris HCl [pH 6.8], 1 M urea, 6.0% 2-mercaptoethanol, 9.3% DTT, 18.0% SDS, 0.06% bromphenol blue, and 30% glycerol). The samples were centrifuged at 425 rcf (2000 rpm) for 30 sec before equal amounts of protein were loaded onto a 4–20% Precise Protein Gel (Pierce, Thermo Scientific, Rockford, IL). The proteins were transferred to an Immobilon-FL® polyvinylidene difluoride membrane (ISEQ00010; Fisher Scientific, Pittsburgh, PA) at room temperature at 100 V. The transfer buffer contained 10% methanol, 24 mM Tris, and 182 mM glycine. Following transfer, the membranes were incubated for 1 h at room temperature (23°C) in fresh SuperBlock (Pierce, Thermo Scientific). Primary antibodies were diluted in blocking solution, and the membranes were incubated with the appropriate antibody overnight at 4°C. The membranes were washed three times for 20 min each in TBS-T, and subsequently incubated with appropriate secondary antibody diluted in blocking solution for 1 h at room temperature. The membranes were again washed three times for 20 min each in TBS-T. Longer washing was used when necessary to reduce background. Western blots for β-actin confirmed equal protein loading.

Primary antibodies used include the following: rabbit anti-Ang-1 (1:800; Invitrogen, Carlsbad, CA), rabbit anti-VEGF

(1:300; Santa Cruz Biotechnology, Santa Cruz, CA), rabbit anti-Iba-1 (0.25 μg/mL; Wako Pure Chemicals, Richmond, VA), and mouse anti-β-actin (1:50,000, ab6276; Abcam, Cambridge, MA). Secondary antibodies used were donkey anti-mouse Alexa 647 (1:5000; Invitrogen), and donkey anti-rabbit (1:5000; Rockland Immunochemicals, Inc., Gilbertsville, PA).

Histochemistry

Viral control animals ($n = 3$) were transcardially perfused with saline followed by 4% paraformaldehyde. The spinal cord was then removed, post-fixed overnight in 4% paraformaldehyde, and then immersed in 30% sucrose plus phosphate-buffered saline (0.1 M PBS) for 2–3 days at 4°C. The spinal cord was trimmed into a 2-cm piece, and embedded in tissue-freezing medium, and frozen at −20°C. The spinal cord segment was sectioned at 30 μm using a cryostat (CM1800; Leica, Bannockburn, IL), and stored at −20°C in tissue-storage medium.

The tissue sections were processed as free-floating, and were incubated in the following primary antibodies: β-galactosidase (biotin) (ab6645, 1:2500; Abcam), myelin basic protein (MBP; MAB381, 1:75; Millipore, Billerica, MA), glial fibrillary acidic protein (GFAP; MAB360, 1:1500; Millipore), and neurofilament-heavy protein (NF-H; AB1991, 1:1000; Millipore). Primary antibodies were diluted with blocking solution (0.1 M PBS containing 5% goat serum and 0.3% Triton X-100).

Appropriate secondary antibodies were used at a dilution of 1:600 in 0.1 M PBS. The following Alexa-Fluor dye–conjugated secondary antibodies were used: streptavidin Alexa Fluor 488, and goat anti-mouse IgG Alexa Fluor 568 (both from Invitrogen). The tissue sections were viewed and captured using a MagnaFire digital camera (Optronics, Goleta, CA) attached to a Leica DMX upright microscope, and the images were collected using MagnaFire software.

Statistical analysis

A one-way analysis of variance (ANOVA) was performed with a *post-hoc* Tukey's multiple comparisons test for Western blot analysis, and differences were considered significant if $p < 0.05$. For BBB locomotor analysis a one-way ANOVA followed by a Bonferroni multiple comparisons test was performed as described previously (Scheff et al., 2002). Data were analyzed using GraphPad Prism 4 software (GraphPad Software, San Diego, CA).

Results

Ang-1 expression profile after spinal cord injury

The Ang-1 expression profile after contusion injury indicated a significant decrease as early as 6 h after injury compared with uninjured control spinal cord tissue. The significant decrease was observed up to 72 h after injury for the acute time points (Fig. 1). We also observed a significant decrease in Ang-1 compared to uninjured tissue in the chronic phase of injury 56 days post-injury (β-actin was used as a loading control). The results support the rationale for supplementing the injured environment with Ang-1 when the

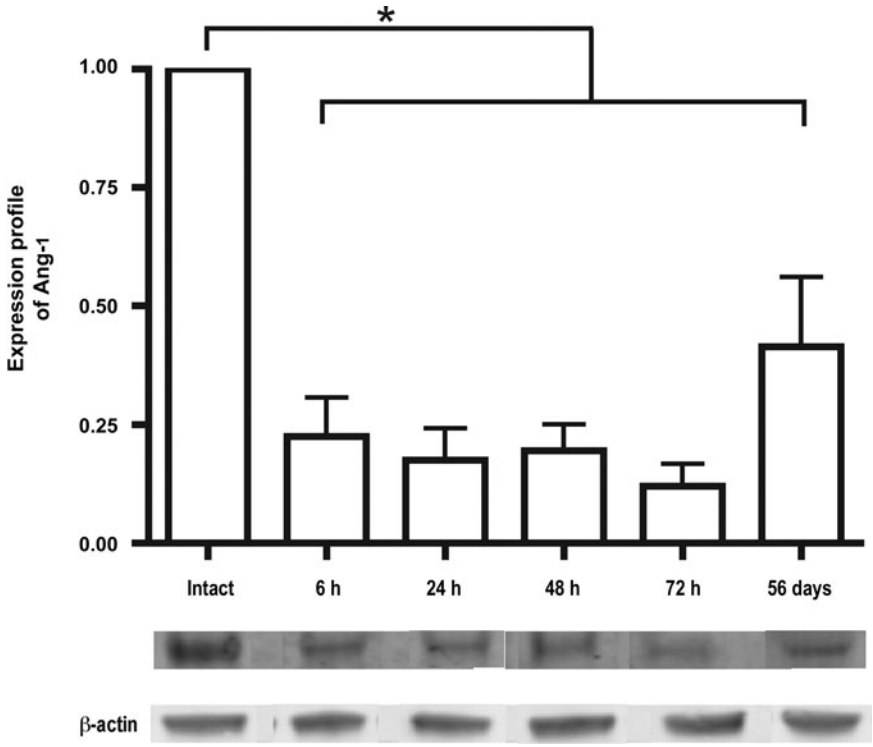

FIG. 1. Protein expression profile of angiopoietin-1 (Ang-1) was determined from the lesion epicenter at 6, 24, 48, and 72 h and 56 days after spinal cord injury, normalized to intact controls. A significant decrease was observed immediately after injury that continued up to 56 days after injury. β-Actin was used as a loading control. Error bars represent standard deviations (*$p < 0.001$).

protein level is low. Our previous study documenting reduced protein expression of $VEGF_{165}$ after SCI also provides the rationale for supplementing the injured environment with $VEGF_{165}$ (Herrera et al., 2009).

AAV delivery of $VEGF_{165}$ and Ang-1 after spinal cord injury

To examine whether there is production of viral vectors in the chronic phase of injury, Western blot analysis was performed on the lesion epicenter at 56 days post-injury. Animals treated with AAV-$VEGF_{165}$ demonstrated a significant increase in VEGF expression compared to the viral control-treated group on day 56 (Fig. 2A). Interestingly, a significant increase in the levels of $VEGF_{165}$ in AAV-Ang-1-treated animals was also observed. Animals treated with AAV-Ang-1 showed a significant increase in Ang-1 (Fig. 2B). A significant increase in Ang-1 expression was also observed in animals treated with AAV-$VEGF_{165}$.

We examined the expression of Iba-1, a macrophage/microglial marker, for infiltration into the lesion site, that in turn may reflect the inflammatory response at 56 days post-injury. Our results indicated no significant difference between any of the viral-treated groups expressing $VEGF_{165}$ and/or Ang-1 compared with viral controls (Fig. 2C). β-Actin was used as a loading control (Fig. 2D). These results indicate that treatment with AAV vectors did not exacerbate the infiltration of activated microglia into the lesion epicenter.

Examination of lesion volume and blood–spinal cord barrier permeability as determined by MRI analysis

To examine the effects of viral treatment on lesion volume, we used anatomical MR imaging (Fig. 3A). Our results indicated that at 56 days post-injury a significant decrease in the hyperintense lesion volume, an indicator of edema and demyelination, was observed in the AAV-Ang-1- and the combined AAV-$VEGF_{165}$/Ang-1-treated groups compared to viral controls (Fig. 3B). There was no significant difference in the hypointense lesion volume, an indicator of hemorrhage and necrosis (Fig. 3C). These data suggest that the sustained expression of $VEGF_{165}$ and Ang-1 improve tissue sparing.

Contrast-enhanced MRI was performed to determine the BSCB breakdown. Our results indicated a reduction in the enhanced area, suggesting the partial restoration of BSCB integrity near the lesion epicenter in animals treated with the combined AAV-$VEGF_{165}$/Ang-1 vectors compared to viral controls (Fig. 3D). No significant change was observed in animals treated with the individual vectors.

Histochemistry of viral expression and open-field locomotor assessment of virally-treated animals

We examined the cell type that was infected by the viral vectors based on LacZ expression. Our results indicated that the viral vectors infected neuronal populations with little observed infection of either astrocyte or oligodendrocyte populations (Fig. 4). Viral vectors also appeared to transduce

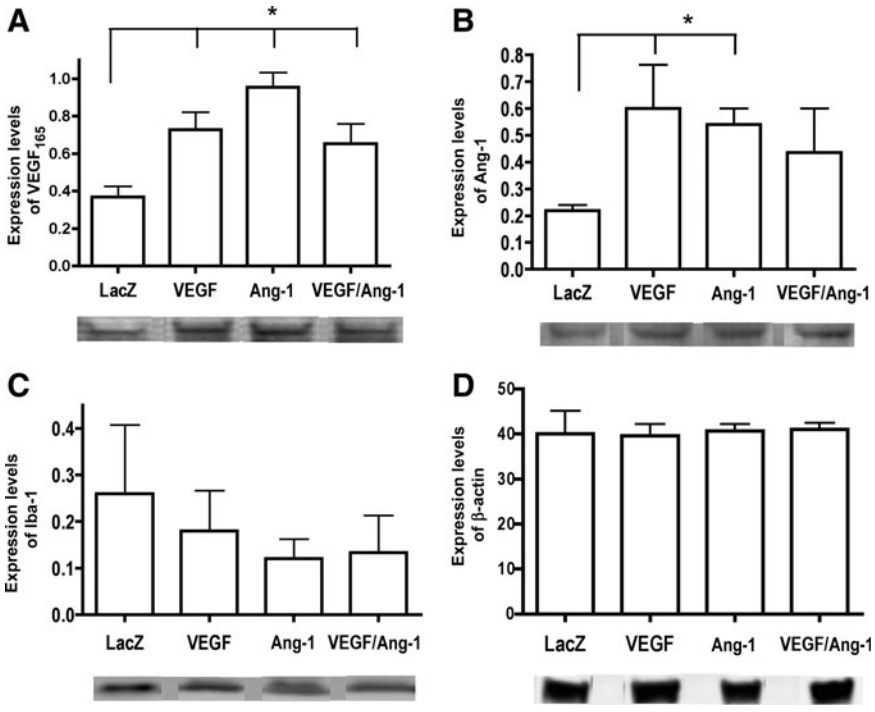

FIG. 2. Adeno-associated virus (AAV) vector expression was determined from the lesion epicenter at 56 days post-injury. **(A)** Expression of vascular endothelial growth factor-165 ($VEGF_{165}$), showing a significant increase in all AAV-treated groups compared to AAV-LacZ viral controls. Error bars represent standard deviations ($^*p = 0.0009$). **(B)** Expression of angiopoietin-1 (Ang-1), indicating a significant increase in the AAV-$VEGF_{165}$- and AAV-Ang-1-treated groups. Error bars represent standard deviations ($^*p = 0.0206$). **(C)** Expression levels of Iba-1, a marker for microglia. No significant difference was observed between treatment groups. Error bars represent standard deviations. **(D)** β-Actin expression to ensure equal concentration of protein loading. No significant differences were observed between groups. Error bars represent standard deviations.

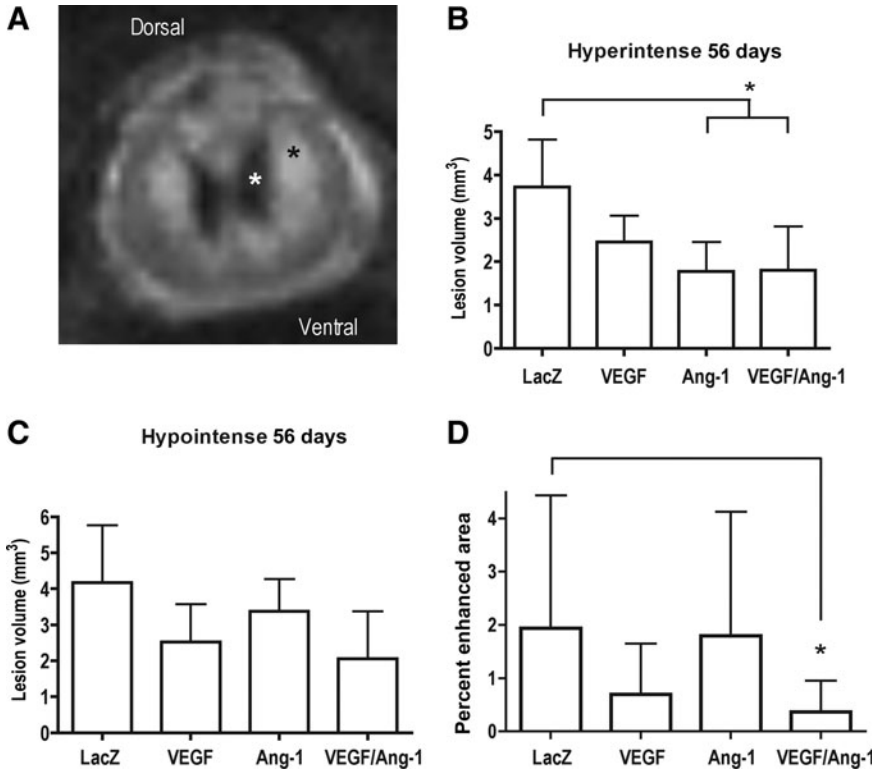

FIG. 3. Magnetic resonance imaging (MRI) analysis of lesion volume and blood–spinal cord barrier permeability at 56 days post-injury. **(A)** T2-weighted RARE image of a typical injured spinal cord showing the hyperintense region (black asterisk) indicating edema and demyelination, and the hypointense region (white asterisk) indicating hemorrhage and necrosis. **(B)** A significant decrease in the hyperintense lesion volume was observed in the AAV-Ang-1- and AAV-$VEGF_{165}$/Ang-1-treated groups. Error bars represent standard deviations ($^*p = 0.0105$). **(C)** No significant decrease was observed in the hypointense lesion volume. **(D)** A significant decrease in the percentage of enhanced area as determined by dynamic contrast imaging was observed in the AAV-$VEGF_{165}$/Ang-1 animals, indicating a reduced general compromise of the blood–spinal cord barrier compared to viral controls. Error bars represent standard deviations ($^*p = 0.0046$; $VEGF_{165}$, vascular endothelial growth factor-165; Ang-1, angiopoietin-1; AAV, adeno-associated virus; RARE, rapid acquisition by relaxation enhancement).

cells beyond the lesion epicenter in both rostral and caudal directions, to a maximum observed distance of 5 mm (data not shown).

To determine whether the sustained expression of either $VEGF_{165}$, Ang-1, or the combined treatment with $VEGF_{165}$ and Ang-1 had an effect on behavioral outcome, the open-field locomotor BBB assay was performed. Our results indicated a significant improvement in BBB scores at 56 days post-SCI only in the combined AAV-$VEGF_{165}$/Ang-1-treated group (Fig. 5).

Discussion

The most important results of this study are: (1) the combined AAV-$VEGF_{165}$/Ang-1 treatment resulted in a significant decrease in the percentage of enhancing area on post-contrast MRI, indicative of improved blood–spinal cord barrier integrity, (2) significant improvements were seen in the BBB scores at 56 days post-injury, and (3) treatment using these AAV vectors did not exacerbate the infiltration of activated microglia into the lesion environment. Our results also indicate that AAV-$VEGF_{165}$, AAV-Ang-1, and combined AAV-$VEGF_{165}$/Ang-1 treatments resulted in reduced hyperintense lesion volume on MRI, indicative of edema and demyelination. Also, though it was not statistically significant, the combined treatment appears to have resulted in the largest reduction in the hypointense lesion volume.

Supplementing the injured environment with $VEGF_{165}$ and Ang-1

Our previous study indicated a significant decrease in the $VEGF_{165}$ splice variant of the VEGF-A family after SCI (Herrera et al., 2009). In the same study we also demonstrated that suppression of $VEGF_{165}$ blocks its neuroprotective effects (Herrera et al., 2009). Thus our rationale was to supplement the injured environment with sustained expression of $VEGF_{165}$ using the AAV delivery system. The use of the AAV system for expressing $VEGF_{165}$ and Ang-1 offers a unique opportunity to study the effects of gene expression for prolonged periods of time *in vivo* without an inflammatory response (Fisher et al., 1997; Snyder et al., 1997; Svensson et al., 1999). There have been studies that examined the therapeutic potential of VEGF in SCI (Liu et al., 2010; Widenfalk et al., 2003). Widenfalk and colleagues demonstrated that exogenous acute intraspinal administration of VEGF-A resulted in improved functional recovery 6 weeks after injury, and increased the amount of spared tissue (Widenfalk et al., 2003). A more recent study by Liu and associates demonstrated that the activation of VEGF-A through AAV-zinc finger protein

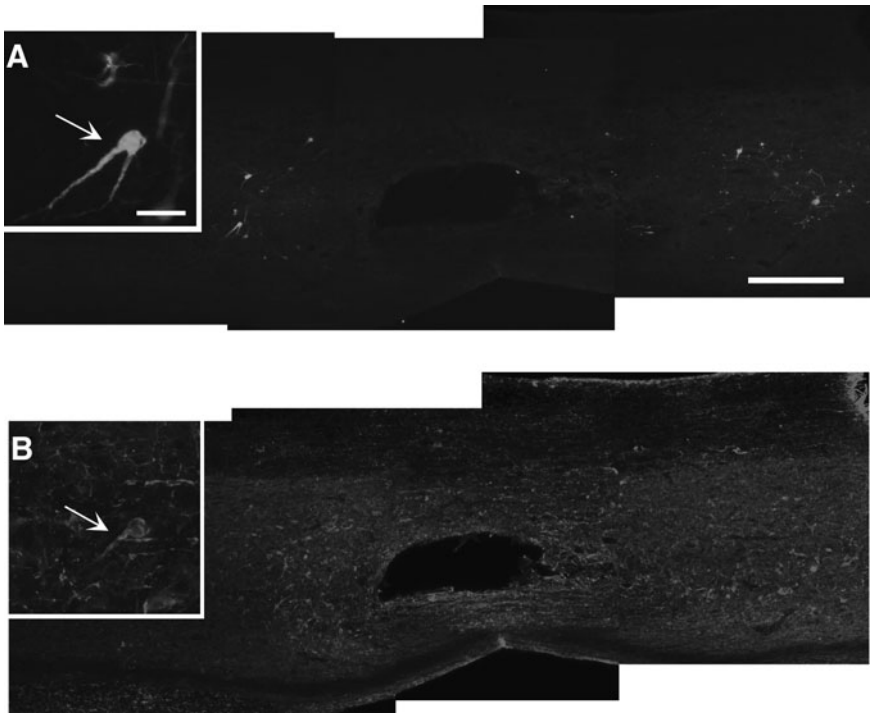

FIG. 4. Representative histology section of an animal treated with AAV-LacZ, indicating that the majority of cells infected with the viral vector are neurons. **(A)** Expression of β-galactosidase, and **(B)** a corresponding section labeled with neurofilament. Inset images show the co-labeling of the transduced AAV-LacZ cells with neurofilament identified with arrows (scale bars = 500 μm in large images, insets = 50 μm; AAV, adeno-associated virus).

transcription activation factors resulted in a reduction of axonal degradation and apoptosis, with enhanced tissue preservation and improved functional recovery 6 weeks after injury (Liu et al., 2010). The later studies, in combination with our current study, support the notion that exogenous administration of $VEGF_{165}$ may have beneficial effects following SCI.

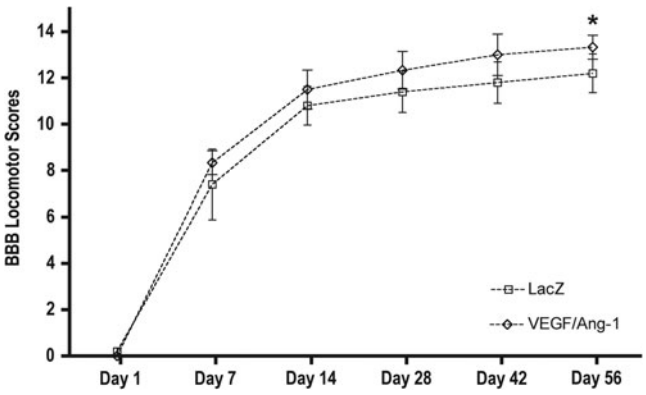

FIG. 5. Basso-Beattie-Bresnahan (BBB) scale scores over time after spinal cord injury (SCI). The BBB scores were significantly higher at 56 days post-injury in animals treated with AAV-$VEGF_{165}$/Ang-1 ($p < 0.05$). Data are presented as mean ± standard deviation. No significant difference was observed between the individually-treated groups compared with viral controls (AAV, adeno-associated virus; $VEGF_{165}$, vascular endothelial growth factor-165).

The use of Ang-1 as a potential therapeutic intervention following SCI has not been widely studied. Ang-1, which is constitutively expressed in the rodent brain (Croll and Wiegand, 2001; Lin et al., 2000; Zhang et al., 2002b), was demonstrated in our study to be significantly decreased after SCI, and appears to remain depressed into the chronic phase of injury. It has also been shown that Ang-1 expression is decreased following blood–brain barrier breakdown (Nourhaghighi et al., 2003). Overexpression of Ang-1 was shown to inhibit the peripheral vascular leakage induced by VEGF or inflammatory agents, suggesting that Ang-1 counters the effect of VEGF on vascular permeability (Thurston et al., 1999, 2000). A study by Zhang and colleagues indicated that virally-delivered Ang-1 given days before ischemic brain injury resulted in reduced vascular leakage and decreased lesion volume (Zhang et al., 2002a). Consistent with a recent article on the therapeutic potential of Ang-1 (Han et al., 2010), our results indicate similar improvements of reduced lesion volume and enhanced functional recovery with Ang-1 treatment.

Synergistic effects of $VEGF_{165}$ and Ang-1

In the current study we examined the effects of combined treatment with $VEGF_{165}$ and Ang-1 acutely after injury. There have been previous studies in other injury models that have examined the therapeutic potential of the combined delivery of AAV-$VEGF_{165}$ and AAV-Ang-1. Gene transfer studies have suggested that the combination of Ang-1 and $VEGF_{165}$ resulted in the formation and/or enhancement of functional neovascularization in models of ischemic stroke (Benest et al., 2006; Chen et al., 2007a, 2007b). Benest and colleagues indicated that a virally-delivered combination of $VEGF_{165}$ and

Ang-1 resulted in a significantly higher number of functionally perfused, larger, less branched, and more mature microvessels (Benest et al., 2006). Results of that study also indicated that the combination of both $VEGF_{165}$ and Ang-1 generated greater enhancement of revascularization and tissue perfusion than either protein used alone. A supporting study by Zacchigna and associates also indicated that vessels formed in response to viral-induced $VEGF_{165}$ alone were observed to be abnormally large and poorly organized in skeletal muscle tissue, while more structured vessels were evident when Ang-1 was expressed together with $VEGF_{165}$ (Zacchigna et al., 2007). Our Gd contrast MRI results indicated that the combined treatment resulted in a reduced percentage of enhancing tissue, suggesting stabilization of disrupted vessels compared to viral controls. The stabilization of the disrupted vasculature likely contributes to the improved functional recovery, as a correlation between compromise of the BSCB and poor motor performance has previously been demonstrated (Patel et al., 2009).

We are currently investigating the possible mechanisms underlying the observations made in our study. The reduction in the general compromise of the BSCB as indicated by the decrease in the percentage of enhanced area seen on contrast MRI might denote a re-establishment of the tight junction network. A recent publication by Lee and colleagues demonstrated that *in vitro,* Ang-1 reduces VEGF-induced brain microvessel permeability by upregulating the tight junction protein zonula occludens-2 (Lee et al., 2009). In addition, occludin, a transmembrane protein expressed exclusively at the tight junction complexes, is induced by Ang-1 expression in brain capillary endothelial cells (Hori et al., 2004). The decrease in the percentage of enhanced area indicating improved BSCB integrity may also upregulate a host of chemoattractants and cellular adhesion molecules that first attract, and then permit neutrophils to transmigrate (diapedese) through the capillaries into the spinal cord tissue. One study found that the peak influx of neutrophils occurs 24 h after experimental SCI (Carlson et al., 1998). Their phagocytic activity can result in free radical production that can lead to lipid peroxidation, cell death, and the release of inflammatory cytokines, such as tumor necrosis factor-α (TNF-α) and the interleukins IL-1α and IL-1β (Means and Anderson, 1983; Taoka and Okajima, 2000). The release of these inflammatory cytokines can in turn exacerbate inflammation in the spinal cord (Popovich and Jones, 2003; Schnell et al., 1999). Restoration of BSCB integrity through the combined treatment with VEGF and Ang-1 may prevent this cascade, impeding the progress of secondary injury.

Our Western blot analysis data indicate that significant increases in Ang-1 and VEGF occurred in the treated animals. As Ang-1 has been demonstrated to stabilize the neovasculature and decrease vascular leakage (Thurston et al., 1999, 2000), the upregulation of Ang-1 is most likely an endogenous response by the neovasculature that was generated by VEGF treatment. Our contrast-enhanced MRI results provide support for this observation. We observed a decrease in the percentage of enhanced area in the AAV-VEGF-treated group. Our Western blot analysis data also indicated a significant increase in VEGF in AAV-Ang-1-treated animals. This was also noted in the contrast MRI results, for which an increasing trend in the percentage of enhanced area was observed in the AAV-Ang-1-treated group. In this instance there may be a unique competitive balance between VEGF and Ang-1. VEGF and Ang-1 work in a coordinated manner during vascular development in embryogenesis; however, a study by Findley and associates demonstrated that VEGF can cleave the Tie-2 receptor, through the phosphoinositide 3-kinase/Akt-dependent pathway, creating a soluble Tie-2 which inactivates Ang-1 (Findley et al., 2007). This may be a novel feedback mechanism in which VEGF downregulates the maturational and remodeling effects of Ang-1, and indicates why VEGF was upregulated in the AAV-Ang-1-treated group.

Further studies are need to examine the mechanisms behind the stabilization of the BSCB, and to determine if stabilization occurs during the acute phase of injury. The signaling mechanisms behind the interplay between VEGF and Ang-1 also need to be examined in the injured environment at both the acute and chronic phases post-injury.

Acknowledgments

This work is supported by NIH/National Institute of Neurological Disorders and Stroke (NINDS) grant NS045624 to P.A.N. The 7-T MRI scanner was funded by the NIH/National Center for Research Resources under the High End Instrumentation Program (grant S10 RR17205-01 to P.A.N.). The NIH is not responsible for the contents of this manuscript.

Author Disclosure Statement

No competing financial interests exist.

References

Arsic, N., Zentilin, L., Zacchigna, S., Santoro, D., Stanta, G., Salvi, A., Sinagra, G., and Giacca, M. (2003). Induction of functional neovascularization by combined VEGF and angiopoietin-1 gene transfer using AAV vectors. Mol. Ther. 7, 450–459.

Basso, D.M., Beattie, M.S., and Bresnahan, J.C. (1995). A sensitive and reliable locomotor rating scale for open field testing in rats. J. Neurotrauma 12, 1–21.

Benest, A.V., Salmon, A.H., Wang, W., Glover, C.P., Uney, J., Harper, S.J., and Bates, D.O. (2006). VEGF and angiopoietin-1 stimulate different angiogenic phenotypes that combine to enhance functional neovascularization in adult tissue. Microcirculation 13, 423–437.

Bilgen, M., Abbe, R., and Narayana, P.A. (2001). Dynamic contrast-enhanced MRI of experimental spinal cord injury: in vivo serial studies. Magn. Reson. Med. 45, 614–622.

Bitto, A., Minutoli, L., Galeano, M.R., Altavilla, D., Polito, F., Fiumara, T., Calo, M., Lo Cascio, P., Zentilin, L., Giacca, M., and Squadrito, F. (2008). Angiopoietin-1 gene transfer improves impaired wound healing in genetically diabetic mice without increasing VEGF expression. Clin. Sci. (Lond.) 114, 707–718.

Bresnahan, J.C., Beattie, M.S., Todd, F.D., 3rd, and Noyes, D.H. (1987). A behavioral and anatomical analysis of spinal cord injury produced by a feedback-controlled impaction device. Exp. Neurol. 95, 548–570.

Carlson, S.L., Parrish, M.E., Springer, J.E., Doty, K., and Dossett, L. (1998). Acute inflammatory response in spinal cord following impact injury. Exp. Neurol. 151, 77–88.

Chen, F., Tan, Z., Dong, C.Y., Chen, X., and Guo, S.F. (2007a). Adeno-associated virus vectors simultaneously encoding VEGF and angiopoietin-1 enhances neovascularization in ischemic rabbit hind-limbs. Acta Pharmacol. Sin. 28, 493–502.

Chen, F., Tan, Z., Dong, C.Y., Li, X., Xie, Y., Wu, Y., Chen, X., and Guo, S. (2007b). Combination of VEGF(165)/Angiopoietin-1 gene and endothelial progenitor cells for therapeutic neovascularization. Eur. J. Pharmacol. 568, 222–230.

Cohen, D.M., Patel, C.B., Ahobila-Vajjula, P., Sundberg, L.M., Chacko, T., Liu, S.J., and Narayana, P.A. (2009). Blood-spinal cord barrier permeability in experimental spinal cord injury: dynamic contrast-enhanced MRI. NMR Biomed. 22, 332–341.

Croll, S.D., and Wiegand, S.J. (2001). Vascular growth factors in cerebral ischemia. Mol. Neurobiol. 23, 121–135.

Croll, S.D., Ransohoff, R.M., Cai, N., Zhang, Q., Martin, F.J., Wei, T., Kasselman, L.J., Kintner, J., Murphy, A.J., Yancopoulos, G.D., and Wiegand, S.J. (2004). VEGF-mediated inflammation precedes angiogenesis in adult brain. Exp. Neurol. 187, 388–402.

Davis, S., Aldrich, T.H., Jones, P.F., Acheson, A., Compton, D.L., Jain, V., Ryan, T.E., Bruno, J., Radziejewski, C., Maisonpierre, P.C., and Yancopoulos, G.D. (1996). Isolation of angiopoietin-1, a ligand for the TIE2 receptor, by secretion-trap expression cloning. Cell 87, 1161–1169.

Deo, A.A., Grill, R.J., Hasan, K.M., and Narayana, P.A. (2006). In vivo serial diffusion tensor imaging of experimental spinal cord injury. J. Neurosci. Res. 83, 801–810.

Fehlings, M.G., Tator, C.H., and Linden, R.D. (1989). The relationships among the severity of spinal cord injury, motor and somatosensory evoked potentials and spinal cord blood flow. Electroencephalogr. Clin. Neurophysiol. 74, 241–259.

Fenyes, D.A., and Narayana, P.A. (1998). In vivo echo-planar imaging of rat spinal cord. Magn. Reson. Imaging 16, 1249–1255.

Ferrara, N., Gerber, H.P., and LeCouter, J. (2003). The biology of VEGF and its receptors. Nat. Med. 9, 669–676.

Findley, C.M., Cudmore, M.J., Ahmed, A., and Kontos, C.D. (2007). VEGF induces Tie2 shedding via a phosphoinositide 3-kinase/Akt dependent pathway to modulate Tie2 signaling. Arterioscler. Thromb. Vasc. Biol. 27, 2619–2626.

Fisher, K.J., Jooss, K., Alston, J., Yang, Y., Haecker, S.E., High, K., Pathak, R., Raper, S.E., and Wilson, J.M. (1997). Recombinant adeno-associated virus for muscle directed gene therapy. Nat. Med. 3, 306–312.

Greenberg, D.A., and Jin, K. (2005). From angiogenesis to neuropathology. Nature 438, 954–959.

Han, S., Arnold, S.A., Sithu, S.D., Mahoney, E.T., Geralds, J.T., Tran, P., Benton, R.L., Maddie, M.A., D'Souza, S.E., Whittemore, S.R., and Hagg, T. (2010). Rescuing vasculature with intravenous angiopoietin-1 and alphavbeta3 integrin peptide is protective after spinal cord injury. Brain 133, 1026–1042.

Harrigan, M.R., Ennis, S.R., Sullivan, S.E., and Keep, R.F. (2003). Effects of intraventricular infusion of vascular endothelial growth factor on cerebral blood flow, edema, and infarct volume. Acta Neurochir. (Wien.) 145, 49–53.

Hausmann, O.N. (2003). Post-traumatic inflammation following spinal cord injury. Spinal Cord 41, 369–378.

Hayashi, T., Abe, K., and Itoyama, Y. (1998). Reduction of ischemic damage by application of vascular endothelial growth factor in rat brain after transient ischemia. J. Cereb. Blood Flow Metab. 18, 887–895.

Hermens, W.T., and Verhaagen, J. (1998). Viral vectors, tools for gene transfer in the nervous system. Prog. Neurobiol. 55, 399–432.

Herrera, J.J., Nesic-Taylor, D.O., and Narayana, P.A. (2009). Reduced vascular endothelial growth factor expression in contusive spinal cord injury. J. Neurotrauma 26, 995–1003.

Holtz, A., Nystrom, B., and Gerdin, B. (1990). Relation between spinal cord blood flow and functional recovery after blocking weight-induced spinal cord injury in rats. Neurosurgery 26, 952–957.

Hori, S., Ohtsuki, S., Hosoya, K., Nakashima, E., Terasaki, T. (2004). A pericyte-derived angiopoietin-1 multimeric complex induces occludin gene expression in brain capillary endothelial cells through Tie-2 activation in vitro. J. Neurochem. 89, 503–513.

Kaya, D., Gursoy-Ozdemir, Y., Yemisci, M., Tuncer, N., Aktan, S., and Dalkara, T. (2005). VEGF protects brain against focal ischemia without increasing blood–brain permeability when administered intracerebroventricularly. J. Cereb. Blood Flow Metab. 25, 1111–1118.

Lang-Lazdunski, L., Matsushita, K., Hirt, L., Waeber, C., Vonsattel, J.P., Moskowitz, M.A., and Dietrich, W.D. (2000). Spinal cord ischemia. Development of a model in the mouse. Stroke 31, 208–213.

Lee, S.W., Kim, W.J., Jun, H.O., Choi, Y.K., and Kim, K.W. (2009). Angiopoietin-1 reduces vascular endothelial growth factor-induced brain endothelial permeability via upregulation of ZO-2. Int. J. Mol. Med. 23, 279–284.

Lin, T.N., Wang, C.K., Cheung, W.M., and Hsu, C.Y. (2000). Induction of angiopoietin and Tie receptor mRNA expression after cerebral ischemia-reperfusion. J. Cereb. Blood Flow Metab. 20, 387–395.

Liu, Y., Figley, S., Spratt, S.K., Lee, G., Ando, D., Surosky, R., and Fehlings, M.G. (2010). An engineered transcription factor which activates VEGF-A enhances recovery after spinal cord injury. Neurobiol. Dis. 37, 384–393.

Means, E.D., and Anderson, D.K. (1983). Neuronophagia by leukocytes in experimental spinal cord injury. J. Neuropathol. Exp. Neurol. 42, 707–719.

Mills, C.D., Grady, J.J., and Hulsebosch, C.E. (2001). Changes in exploratory behavior as a measure of chronic central pain following spinal cord injury. J. Neurotrauma 18, 1091–1105.

Neufeld, G., Cohen, T., Gengrinovitch, S., and Poltorak, Z. (1999). Vascular endothelial growth factor (VEGF) and its receptors. FASEB J. 13, 9–22.

Nourhaghighi, N., Teichert-Kuliszewska, K., Davis, J., Stewart, D.J., and Nag, S. (2003). Altered expression of angiopoietins during blood-brain barrier breakdown and angiogenesis. Lab. Invest. 83, 1211–1222.

Patel, C.B., Cohen, D.M., Ahobila-Vajjula, P., Sundberg, L.M., Chacko, T., and Narayana, P.A. (2009). Effect of VEGF Treatment on the blood-spinal cord barrier permeability in experimental spinal cord injury: Dynamic contrast-enhanced magnetic resonance imaging. J. Neurotrauma 26, 1005–1016.

Peng, X.M., Zhou, Z.G., Glorioso, J.C., Fink, D.J., and Mata, M. (2006). Tumor necrosis factor-alpha contributes to below-level neuropathic pain after spinal cord injury. Ann. Neurol. 59, 843–851.

Popovich, P.G., and Jones, T.B. (2003). Manipulating neuroinflammatory reactions in the injured spinal cord: back to basics. Trends Pharmacol. Sci. 24, 13–17.

Proescholdt, M.A., Jacobson, S., Tresser, N., Oldfield, E.H., and Merrill, M.J. (2002). Vascular endothelial growth factor is expressed in multiple sclerosis plaques and can induce inflammatory lesions in experimental allergic encephalomyelitis rats. J. Neuropathol. Exp. Neurol. 61, 914–925.

Rivlin, A.S., and Tator, C.H. (1977). Objective clinical assessment of motor function after experimental spinal cord injury in the rat. J. Neurosurg. 47, 577–581.

Scheff, S.W., Rabchevsky, A.G., Fugaccia, I., Main, J.A., and Lumpp, J.E, Jr. (2003). Experimental modeling of spinal cord injury: characterization of a force-defined injury device. J. Neurotrauma 20, 179–193.

Scheff, S.W., Saucier, D.A., and Cain, M.E. (2002). A statistical method for analyzing rating scale data: the BBB locomotor score. J. Neurotrauma 19, 1251–1260.

Schnell, L., Fearn, S., Klassen, H., Schwab, M.E., and Perry, V.H. (1999). Acute inflammatory responses to mechanical lesions in the CNS: differences between brain and spinal cord. Eur. J. Neurosci. 11, 3648–3658.

Snyder, R.O., Spratt, S.K., Lagarde, C., Bohl, D., Kaspar, B., Sloan, B., Cohen, L.K., and Danos, O. (1997). Efficient and stable adeno-associated virus-mediated transduction in the skeletal muscle of adult immunocompetent mice. Hum. Gene Ther. 8, 1891–1900.

Suidan, G.L., Dickerson, J.W., Chen, Y., McDole, J.R., Tripathi, P., Pirko, I., Seroogy, K.B., and Johnson, A.J. (2010). CD8 T cell-initiated vascular endothelial growth factor expression promotes central nervous system vascular permeability under neuroinflammatory conditions. J. Immunol. 184, 1031–1040.

Sun, Y., Jin, K., Xie, L., Childs, J., Mao, X.O., Logvinova, A., and Greenberg, D.A. (2003). VEGF-induced neuroprotection, neurogenesis, and angiogenesis after focal cerebral ischemia. J. Clin. Invest. 111, 1843–1851.

Suri, C., Jones, P.F., Patan, S., Bartunkova, S., Maisonpierre, P.C., Davis, S., Sato, T.N., and Yancopoulos, G.D. (1996). Requisite role of angiopoietin-1, a ligand for the TIE2 receptor, during embryonic angiogenesis. Cell 87, 1171–1180.

Svensson, E.C., Marshall, D.J., Woodard, K., Lin, H., Jiang, F., Chu, L., and Leiden, J.M. (1999). Efficient and stable transduction of cardiomyocytes after intramyocardial injection or intracoronary perfusion with recombinant adeno-associated virus vectors. Circulation 99, 201–205.

Taoka, Y., and Okajima, K. (2000). Role of leukocytes in spinal cord injury in rats. J. Neurotrauma 17, 219–229.

Tator, C.H., and Fehlings, M.G. (1991). Review of the secondary injury theory of acute spinal cord trauma with emphasis on vascular mechanisms. J. Neurosurg. 75, 15–26.

Tator, C.H. (1991). Review of experimental spinal cord injury with emphasis on the local and systemic circulatory effects. Neurochirurgie 37, 291–302.

Thurston, G., Rudge, J.S., Ioffe, E., Zhou, H., Ross, L., Croll, S.D., Glazer, N., Holash, J., McDonald, D.M., and Yancopoulos, G.D. (2000). Angiopoietin-1 protects the adult vasculature against plasma leakage. Nat. Med. 6, 460–463.

Thurston, G., Suri, C., Smith, K., McClain, J., Sato, T.N., Yancopoulos, G.D., and McDonald, D.M. (1999). Leakage-resistant blood vessels in mice transgenically overexpressing angiopoietin-1. Science 286, 2511–2514.

Tofts, P.S., Brix, G., Buckley, D.L., Evelhoch, J.L., Henderson, E., Knopp, M.V., Larsson, H.B., Lee, T.Y., Mayr, N.A., Parker, G.J., Port, R.E., Taylor, J., and Weisskoff, R.M. (1999). Estimating kinetic parameters from dynamic contrast-enhanced T(1)-weighted MRI of a diffusable tracer: standardized quantities and symbols. J. Magn. Reson. Imaging. 10, 223–232.

Weirich, S.D., Cotler, H.B., Narayana, P.A., Hazle, J.D., Jackson, E.F., Coupe, K.J., McDonald, C.L., Langford, L.A., and Harris, J.H., Jr. (1990). Histopathologic correlation of magnetic resonance imaging signal patterns in a spinal cord injury model. Spine 15, 630–638.

Widenfalk, J., Lipson, A., Jubran, M., Hofstetter, C., Ebendal, T., Cao, Y., and Olson, L. (2003). Vascular endothelial growth factor improves functional outcome and decreases secondary degeneration in experimental spinal cord contusion injury. Neuroscience 120, 951–960.

Zacchigna, S., Tasciotti, E., Kusmic, C., Arsic, N., Sorace, O., Marini, C., Marzullo, P., Pardini, S., Petroni, D., Pattarini, L., Moimas, S., Giacca, M., and Sambuceti, G. (2007). In vivo imaging shows abnormal function of vascular endothelial growth factor-induced vasculature. Hum. Gene Ther. 18, 515–524.

Zhang, Z.G., Zhang, L., Croll, S.D., and Chopp, M. (2002a). Angiopoietin-1 reduces cerebral blood vessel leakage and ischemic lesion volume after focal cerebral embolic ischemia in mice. Neuroscience 113, 683–687.

Zhang, Z.G., Zhang, L., Tsang, W., Soltanian-Zadeh, H., Morris, D., Zhang, R., Goussev, A., Powers, C., Yeich, T., and Chopp, M. (2002b). Correlation of VEGF and angiopoietin expression with disruption of blood-brain barrier and angiogenesis after focal cerebral ischemia. J. Cereb. Blood Flow Metab. 22, 379–392.

Zhao, Y., Li, Z., Wang, R., Wei, J., Li, G., and Zhao, H. (2009). Angiopoietin 1 counteracts vascular endothelial growth factor-induced blood-brain barrier permeability and alleviates ischemic injury in the early stages of transient focal cerebral ischemia in rats. Neurol. Res. 32, 748–755.

Address correspondence to:
Juan J. Herrera, Ph.D.
Diagnostic and Interventional Imaging
The University of Texas Health Science Center at Houston
6431 Fannin
MSE R102F
Houston, TX 77030

E-mail: Juan.Herrera@uth.tmc.edu